A numerical model for real-time monitoring of urban air quality

A.V. Starchenko and D.A. Belikov

Tomsk State University

A prognostic model based on assimilation of meteorological observations is proposed for the air quality control in an urban area. A short-term forecast of the urban weather is obtained using a one-dimensional unsteady model of the atmospheric boundary layer. High reliability of meteorological forecast is achieved due to assimilation of meteorological data (wind velocity, temperature, and humidity) in the model. The model predicts a detailed pattern of the vertical distribution of horizontal wind components and turbulent parameters, which are very important in simulating the pollution dispersion in the near-surface air. Pollution transport through an urban air basin is predicted based on the equations of spatial transport of harmful species chosen for study. The following pollution sources are considered: stacks of industrial and heat-and-power production plants (point sources), traffic (linear sources), and large industrial area (area sources). The problem is solved numerically using the finite volume method and the factorization method. To speed up the solution of the problem, we used high performance computers of TSU and IAO SB RAS. The parallel computational algorithm used for numerical solution is based on domain decomposition. The model developed is applied to prediction of air quality in Tomsk for several chosen dates of 2000. The results of comparison of predictions and observations demonstrate applicability of the proposed approach, whose main advantage is high performance in forecasting of air pollution distribution over urban areas.

Introduction

The distribution of concentration of the primary and secondary pollutants of the urban air is calculated using transport models, which describe the substance transport by wind, substance dispersal due to turbulence, and possible chemical reactions. To take into account the first two factors, we have to have detailed information on the structure and dynamics of the atmospheric boundary layer parameters over a city. The most complete pattern of atmospheric processes can be obtained from spatial prognostic mesoscale models in combination with the use of observation data.[1,2] Nevertheless, even at such detailed and theoretically justified approach to prediction of the environmental dynamics, the quality of such prediction may happen to be low because of incomplete information on the initial state of the system modeled and uncertainty in its parameters. Besides, since numerical calculations take a lot of computer resources even on modern supercomputers, the use of three-dimensional unsteady models of the atmospheric boundary layer is now restricted to only scenario analysis for revealing the main disturbing factors of the system under study.

For real-time calculation of the pollutant content in the urban air, it is also possible to make use of simplified empirical models that are based on the results of observations. The simplest method of estimating the distribution of the wind velocity and the turbulent diffusion coefficient is application of power dependences on the vertical coordinate.[3,4] In this case, the exponent depends on the atmospheric stratification. These models can be used if only the observations of the atmospheric conditions are available.

Another one method to describe quantitatively the behavior of the meteorological characteristics and the vertical turbulent structure of the atmospheric boundary layer is the use of one-dimensional unsteady models. In the 70–80s this approach was already applied to development of theories of atmospheric turbulence. In some papers, one-dimensional unsteady models of the atmospheric boundary layer (ABL) serve as a basis for determination of the vertical profiles of the horizontal wind components and turbulent characteristics, which were then used to study the admixture transport in the atmospheric surface layer over thermally and orographically homogeneous terrain.[5,6]

One-dimensional models are simplified versions of spatial models, in which the meteorological parameters (air temperature and humidity, wind velocity and direction) are believed constant in the horizontal plane and only their variations with height and in time are taken into consideration. In real ABL the horizontal component of the wind velocity usually far exceeds the vertical one, and diffusion processes are more intense in the vertical direction. Therefore, the transition to the one-dimensional model can be considered as a result of simplification of a complex three-dimensional hydrostatic mesoscale model, whose numerical realization requires considerable computer resources even at the low vertical resolution.

At the same time, one-dimensional models based on the data of atmospheric observations have high vertical and time resolution, and for local territories they satisfactorily describe the diurnal variability of the meteorological parameters. Since these models take into account the laws of conservation, they have the undoubted advantage over the simplest power models of turbulent diffusion and horizontal wind components, but compare well with the latter in the computational time. Besides, one-dimensional unsteady models take into account the diurnal dynamics of the turbulent structure. In combination, for instance, with the diagnostic model of wind,[7] this allows consideration of the effect of mesoscale features connected with inhomogeneous properties of the terrain on the pollutant transport and dispersal in the atmospheric surface layer.

One-dimensional model

To describe the field of horizontal wind and turbulent structure of the atmosphere that is very important for adequate representation of the pollutant transport, the laws of conservation of the momentum and energy in the differential form were used. The following assumptions were accepted:

– the air density was assumed depending on the basic values of pressure and temperature of the atmospheric boundary layer, and density variations with temperature were taken into account only when modeling turbulence;

– the numerical model ignored the processes associated with the phase transformations of water vapor in the atmosphere and modification of thermal fluxes passing through the atmosphere;

– the processes of molecular diffusion were believed insignificant as compared with the turbulent exchange;

– the meteorological parameters (horizontal velocity components and temperature) were taken varying only with time and height.

With the allowance for the above assumptions, the equations for the mean wind components and the potential temperature and humidity have the form[8]:

$$\frac{\partial U}{\partial t} = -\frac{\partial}{\partial z}\langle uw \rangle + f(V - V_g), \qquad (1)$$

$$\frac{\partial V}{\partial t} = -\frac{\partial}{\partial z}\langle vw \rangle - f(U - U_g), \qquad (2)$$

$$\frac{\partial \Theta}{\partial t} = -\frac{\partial}{\partial z}\langle \theta w \rangle, \qquad (3)$$

$$\frac{\partial q}{\partial t} = -\frac{\partial}{\partial z}\langle qw \rangle, \qquad (4)$$

where U and V are the components of the horizontal wind velocity in the atmospheric boundary layer ($W \cong 0$), the axis Ox is directed eastward, Oy is looking northward; u, v, w are the pulsation components of the horizontal and vertical velocity, respectively; $\langle uw \rangle$, $\langle vw \rangle$, $\langle \theta w \rangle$, $\langle qw \rangle$ are the turbulent correlations of pulsations of the vertical and horizontal velocity components and temperature or humidity;

$$(U_g, \quad V_g) = \frac{1}{\rho f}\left(-\frac{\partial p}{\partial y}, \frac{\partial p}{\partial x}\right)$$

are the components of the geostrophic wind, ρ is the density; t is time, z is the vertical coordinate; $\Theta = T (P_0/P)^{R/c_p}$ is the potential temperature; $P_0 = 1.013 \cdot 10^5$ N/m^2, c_p is the specific heat of air at constant pressure, T is the absolute temperature, R is the universal gas constant; $f = 2\Omega \sin\psi$ is the Coriolis parameter, ψ is the geographic latitude of the point under consideration, Ω is the angular velocity of the Earth revolution.

Since the lower atmospheric layer up to the height of 1000–1500 m is characterized by turbulent mixing that significantly affects the structure of the atmospheric boundary layer, particular attention is paid to modeling of turbulence. Here we use the "$E - l$" model of turbulence that includes the transfer equations for energy and the scale of turbulent pulsations and algebraic equations for Reynolds stresses and turbulent heat fluxes[8]:

$$\frac{\partial E}{\partial t} = -\langle uw \rangle \frac{\partial U}{\partial z} - \langle vw \rangle \frac{\partial V}{\partial z} + \frac{g}{\Theta}\langle \theta w \rangle +$$
$$+ \frac{\partial}{\partial z}\left(\sigma_e \sqrt{E}l\frac{\partial k}{\partial z}\right) - \frac{C_D E^{\frac{3}{2}}}{l}, \qquad (5)$$

$$\frac{\partial l}{\partial t} = C_{L1}\left(-\langle uw \rangle \frac{\partial U}{\partial z} - \langle vw \rangle \frac{\partial V}{\partial z} + \frac{g}{\Theta}\langle \theta w \rangle\right)\frac{l}{E} +$$
$$+ \frac{\partial}{\partial z}\left(\sigma_e \sqrt{E}l\frac{\partial l}{\partial z}\right) + C_{L2}\sqrt{E}\left[1 - \left(\frac{l}{\kappa z}\right)^2\right], \qquad (6)$$

$$\left[\langle uw \rangle, \langle vw \rangle, \langle \theta w \rangle\right] = -F_{m,h}\sqrt{E}l\left[\frac{\partial U}{\partial z}, \frac{\partial V}{\partial z}, \frac{\partial \Theta}{\partial z}\right]. \qquad (7)$$

Here $E = 0.5 (\langle u^2 \rangle + \langle v^2 \rangle + \langle w^2 \rangle)$ is the kinetic energy of turbulence; l is the scale of turbulence; $\sigma_e = 0.54$; $C_{L1} = -0.12$; $C_{L2} = 0.2$; $C_D = 0.19$; $\kappa = 0.4$. F_m and F_h are the functions of local turbulent characteristics.[8]

The boundary conditions for the Eqs. (1)–(6) were formulated as follows[8]:

at $z = z_1 \gg z_0$

$$U = \frac{v_*}{\kappa}f_u(\zeta_1)\cos\beta; \; V = \frac{v_*}{\kappa}f_u(\zeta_1)\sin\beta;$$

$$\Theta = \Theta_1^{obs}(t); \; q = q_1^{obs}(t); \; E = v_*^2 f_k(\zeta_1); \; l = \kappa z f_l(\zeta_1);$$

at $z = H$

$$\frac{\partial U}{\partial z} = \frac{\partial V}{\partial z} = \frac{\partial E}{\partial z} = \frac{\partial l}{\partial z} = \frac{\partial q}{\partial z} = 0; \; \frac{\partial \Theta}{\partial z} = \gamma.$$

Here z_0, z_1, H are the roughness height, the height of the first computational level, and the height of the computational domain; v_* is the dynamic velocity; f_u, f_k, f_l are the empirical functions; $\zeta = z/L$, L is the Monin–Obukhov scale.

The initial conditions for Eqs. (1)–(4) were specified using the observational data on the vertical structure of the atmospheric boundary layer. For turbulent characteristics, the initial profiles were pre-calculated by the above model at a fixed average dynamics and temperature ABL parameters.

Use of observations in modeling

To improve the quality of calculated results on the meteorological fields, various methods of assimilation of observations into models were used.

A. Meteorological measurements, both ground-based and obtained with remote sensing facilities (sodars, lidars, radars, etc), were used for reconstruction of the vertical structure of the atmospheric boundary layer (vertical dependence of humidity, potential temperature, and horizontal wind velocity components)[9]:

$$\varphi_S(z) = \varphi_{sound}^*(z)\,[1 - \chi(z)] +$$
$$+ \,\varphi_{ground}\,\chi(z)\,\min\,[1.0;\,(z/50)^k],$$

where $\varphi_{sound}^*(z)$ is the function constructed through spline-interpolation of the measured values of $\varphi_{sound}(z_i)$; φ_{ground} are the measurement data on near surface quantities; k depends on the atmospheric stratification ($k = 0$ for $\varphi = \Theta$, q);

$$\chi(z) = 1 - \min\,[1.0;\,(z/200)^2].$$

Thus constructed profiles of $\varphi_S(z)$ were used in specifying the initial distributions of the velocity, temperature, and humidity.

Besides, the obtained vertical distributions were used to correct the numerically calculated results by observations. For this purpose, Eqs. (1)–(4) were complemented with terms of the following form[10]:
$-[\varphi(t,z) - \overline{\varphi}_S(t,z)]/\tau_S$.
Here

$$\overline{\varphi}_S(t,z) = \varphi_{S1}(z) + \frac{\varphi_{S2}(z) - \varphi_{S1}(z)}{\tau_S}(t - t_1)\,,$$

$t_1 \le t \le t_2$; $\tau_S = t_2 - t_1$; $\varphi_{S1}(z)$ and $\varphi_{S2}(z)$ are the vertical profiles reconstructed for the moments t_1 and t_1 in time.

B. Observations of variations of the surface temperature and humidity were directly used by the model as boundary conditions for Eqs. (3) and (4). As compared to observations of the ABL vertical structure, the frequency of measurements of the near-surface temperature and humidity is higher (in our calculations we used the hourly measured values). The use of air temperature and humidity observations as boundary conditions significantly simplifies the problem formulation, removing the need in modeling the intensity of heat and moisture exchange on the surface.[6]

C. The effect of synoptic meteorology in local dynamic processes is taken into account by specifying the components of the geostrophic wind U_g and V_g. In this paper, the geostrophic wind is estimated using modified Shnaidman technique,[11] which is based on observations of the near-surface atmospheric pressure at the neighboring large weather stations (Kolpashevo, Novosibirsk, Kemerovo, and Tomsk).[12]

The main steps of this technique are the following:

1. The near-surface pressure measured at certain time at the height above the sea level of the ith weather station is re-calculated to the height above the sea level z_* of the site, for which the atmospheric processes are modeled:

$$p_i(z_*) = p_i(z_i)\exp(g(z_i - z_*)/RT_i)\,,\; i = 1,2,\ldots,n$$

(p_i, T_i are the pressure and temperature measured at the height z_i above the sea level for the ith station).

2. Then for a set of the data $p_i(z_*) = f(x_i, y_i)$ ((x_i,y_i) are the coordinates of the weather stations) ($i = 1, \ldots, n$) the least-squares method is applied to draw the dependence approximating the synoptic pressure distribution

$$\tilde{p}(x,y,z_*) = p_* + d_x(x_* - x) + d_y(y_* - y),$$
$$d_x, d_y \text{ are constants.}$$

3. Then the derivatives at $x = x_*$, $y = y_*$ are calculated as

$$-\frac{1}{\rho}\frac{\partial \tilde{p}}{\partial x} = \frac{RT_* d_x}{p_*};\; -\frac{1}{\rho}\frac{\partial \tilde{p}}{\partial y} = \frac{RT_* d_y}{p_*}\,.$$

4. The pressure gradients at different time are used to determine the geostrophic wind components $U_g(t)$ and $V_g(t)$ from the Ekman equations:

$$\frac{\partial U_g}{\partial t} = fV_g - \frac{1}{\rho}\frac{\partial \tilde{p}}{\partial x},$$

$$\frac{\partial V_g}{\partial t} = -fU_g - \frac{1}{\rho}\frac{\partial \tilde{p}}{\partial y}.$$

Modeling of pollutant transport

In this paper, to calculate the transport, dispersal, and transformation of minor constituents of the surface atmosphere, we use the prognostic advection-diffusion equation[3]:

$$\frac{\partial c_j}{\partial t} + \frac{\partial U c_j}{\partial x} + \frac{\partial V c_j}{\partial y} + \frac{\partial W_j c_j}{\partial z} = \frac{\partial}{\partial x}\left(K_Z^h \frac{\partial c_j}{\partial x}\right) +$$

$$+\frac{\partial}{\partial y}\left(K_Z^h \frac{\partial c_j}{\partial y}\right) + \frac{\partial}{\partial z}\left(K_Z^h \frac{\partial c_j}{\partial z}\right) + Q_j,\; j = 1,\ldots,s. \quad (8)$$

Here c_j is the concentration of the jth constituent; Q_j is the source term modeling the income of pollutants and change of their concentration due to chemical reactions; W_j is the velocity of vertical motion of the jth constituent; s is the number of constituents; $K_Z^h = F_h \sqrt{El}$.   Simple   gradient conditions at the side, upper, and lower boundaries of the domain of investigations are used as boundary conditions.

Method of calculation

The problem presented by Eqs. (1) to (8) with the boundary and initial conditions was solved numerically by the finite-difference method on a grid, which became denser in the direction to the surface. Densening was specified in such a way that the ratio of the size of neighboring grids kept constant. The position of the first computational level was significantly higher than the roughness height of the surface z_0. The discrete version of the differential problem (1)–(7) was constructed with the second order of approximation in time and height. The obtained systems of difference equations were solved by the effective fitting method.[13]

The spatial unsteady equations (8) were solved numerically for a parallelepiped with numerous linear, point, and area emission sources and high-altitude point sources. In the domain of investigation, which covers the city and its suburbs, a finite-difference grid with the constant horizontal dimensions of cells and varying vertical dimensions decreasing in the direction toward the surface was constructed. Differential operators in Eqs. (8) were approximated with the second order of accuracy in coordinates and the first order of accuracy in time using explicit difference schemes for all the terms of the equation except for the vertical diffusion. This method of discretization of the differential problem allows us to solve problems arising because of nonlinearity of Eqs. (8) and to significantly accelerate obtaining the solution because of the use of the efficient sweep method with acceptable restriction of the time step. The advective terms of transport equations (8) are approximated using monotonized upstream Van Leer scheme[14] that does not allow appearance of unreal concentration values.

In the proposed approximate model of atmospheric processes and pollution transport in urban air, the main computational load is associated with solution of 3D unsteady equations (8). The need in monitoring of the air quality indicates the necessity of obtaining a detailed pattern of the pollutant distribution in the surface urban air; therefore, the computational grid should have the highest density of nodes in this domain of investigation. Besides, to take into account chemical reactions giving rise to secondary pollutants of the urban air basin (ozone, styrene), it is necessary to consider the transport and dispersal of a large

number of pollutants. These conditions of numerical calculations force us to use high-performance computers, in particular, multiprocessor cluster systems of the Institute of Atmospheric Optics SB RAS (http://cluster.iao.ru) and of the Tomsk State University (http://cluster.tsu.ru) with the MPI (Message Passing Interface) installed.[15]

Numerical solution of Eqs. (8) was paralleled using the geometric principle of data decomposition. The entire domain was divided into identical regions. In this study, the domain parallelepiped ($-L_x/2 \le x \le L_x/2$; $-L_y/2 \le y \le L_y/2$; $0 \le z \le L_z$) was cut by the sections y = const and the data from every region were assigned to the corresponding processor element. All the grid values of the concentration $(c_j)_{k,l,m}^{n+1}$ were uniformly distributed over the computational nodes of the distributed-memory multiprocessor system. Inside every region, the grid equations obtained from discretization of Eqs. (8) were solved simultaneously by the sweep method. However, because of the selected difference mask, two grid values of the concentration from the neighboring region are needed when calculating the concentrations along the near-boundary grid line (near the upper or lower boundary of the region) (see Fig. 1).
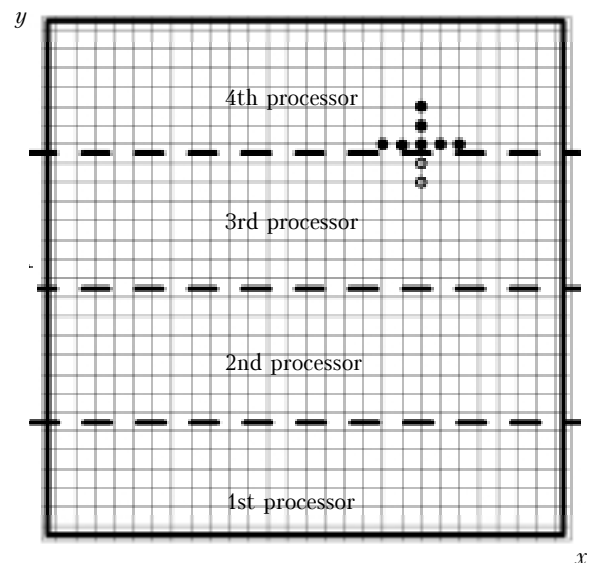
Fig. 1. Computational grid in the plane xOy with indicated distribution of regions over four processors. The difference mask is shown on the near-boundary grid line. Open circles indicate the grid values to be received from the neighboring processor.

Therefore, for the correct operation of the parallel program, it is necessary to organize the exchange of near-boundary grid values between the processors. This task was completed using MPI_SendRecv library function. Besides, for preparation of parallel computations, the following Message Passing Interface library functions were invoked: MPI_Bcast and MPI_Scatter.

Computational conditions and discussion

The method proposed for calculating the distribution of the main pollutants using high-performance computers was adapted to account for conditions of Tomsk. Four components of atmospheric pollution were considered, namely, dust, CO, SO_2, and NO_2, and 119 linear, 12 area, and 338 point emission sources located at Tomsk territory were considered (Fig. 2). In the calculations, it was assumed that these components are chemically inert. The calculations were performed on the $100 \times 100 \times 50$ grid with the 30 s step for determination of the atmospheric parameters and 15 s step for calculation of the distribution of the main pollutants in the urban air basin.

The intensity of traffic emissions depended on time and was calculated by the following law:

$$Q/Q_0 = \begin{cases} 0.1 & 0 \le t(h) \le 6, \\ 0.1 + 1.9\sin\left(\pi\dfrac{t(h)-6}{18}\right), & 6 \le t(h) \le 24, \end{cases} \quad (9)$$

where Q_0 is the diurnally mean intensity of emissions from a linear source; $t(h)$ is local time, h.

Figure 3 depicts the gain in time provided by the parallel algorithm considered above when running the corresponding program on the cluster system of the Tomsk State University (nine two-processor computers with Pentium III 650 MHz processors, RAM 256 Mb connected by Fast Ethernet 100 Mbit). The gain is understood as a ratio of time needed for execution of the program on a single processor to the time needed for solution of the problem on p processors. It can be seen from Fig. 3 that when the parallel program is run on 10 processors of the TSU cluster at the above parameters, the gain of more than six can be achieved. At the same time, the efficiency of the parallel program (the ratio of the time gain to the number of processors involved) decreases with increasing p. This is explained by the fact that at the fixed number of nodes of the finite-difference grid the ratio of computations to the number of exchanges decreases. The comparative calculations made on the IAO multiprocessor system (10 two-processor computers with Pentium III 1 GHz, RAM 1 Gb, Gigabit Ethernet 1 Gbit) showed that getting the two-day model distribution of the four main urban air pollutants on 10 processors takes a little bit more than 3 h.
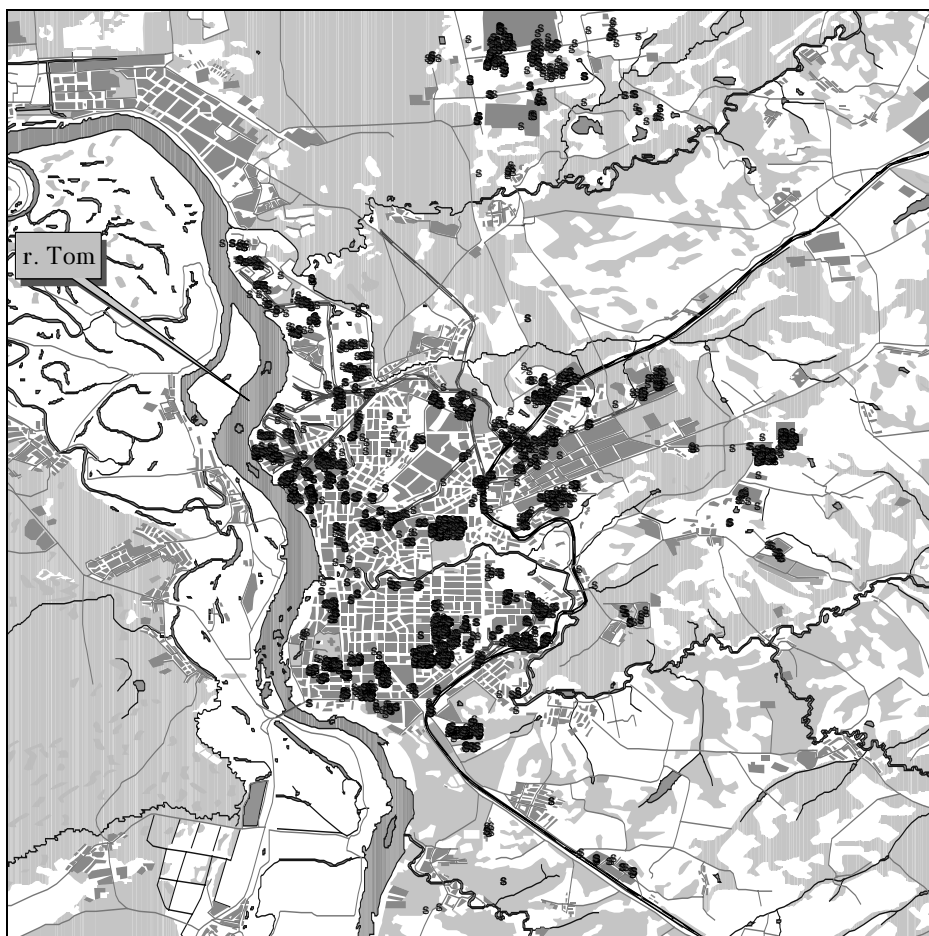
Fig. 2. Distribution of steady-state sources of pollution of Tomsk atmosphere.
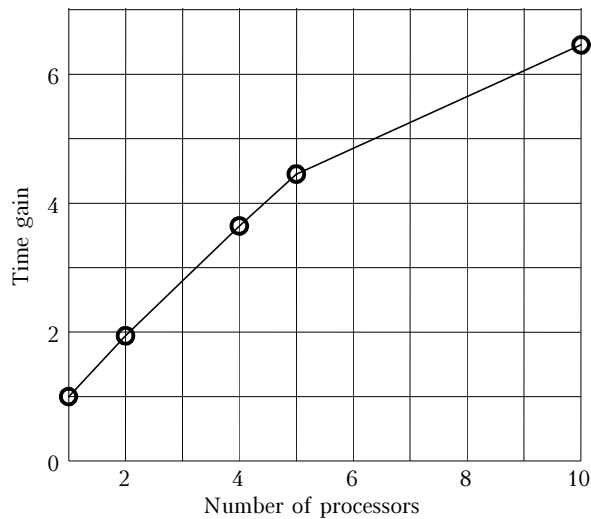
Fig. 3. Time gain of the parallel computational process vs. the number of processors involved.

To prove that the model described above can be applied to description of the real pattern of the urban air quality, it was tested widely. First, the results given by the one-dimensional model of the atmospheric boundary layer were compared with the basic data (experimental and theoretical) for the neutral, steady, and convective state of the planetary boundary layer,[8,16,17] and a good agreement was obtained.

Second, this model was applied for selected dates of 2000 (January 10–11, March 16–17, June 29–30, and September 7–8) for Tomsk conditions. The results obtained were compared with the results calculated by the mesoscale non-hydrostatic model of the atmospheric boundary layer[2] and the observations obtained earlier. Figures 4–7 compare the calculated and measured speed and directions of the surface wind in Tomsk on the selected days. Open circles present wind observations at the TOR station of the Institute of Atmospheric Optics located in the eastern suburbs of Tomsk (http://meteo.iao.ru). Half-open circles present the measurements of the RF State Hydrology & Meteorology Center[12] at the weather station located in southern suburbs of Tomsk. Note that these data were not assimilated by the model and were considered only as control ones. The calculated wind speed and directions obtained by the 3D mesoscale non-hydrostatic model[2] are presented for the Tomsk downtown area. On the whole, good agreement with the observations on the wind speed and direction in Tomsk was obtained.

Besides, the proposed model (1)–(7) in combination with the Euler model of pollutant transport and dispersal (8) was used to estimate the CO distribution over Tomsk. In calculations for steady sources (industrial plants), the values of the emission intensity given by administrative bodies on environmental protection were used. The traffic emissions were estimated from the traffic intensity on particular highways using empirical dependence (9).
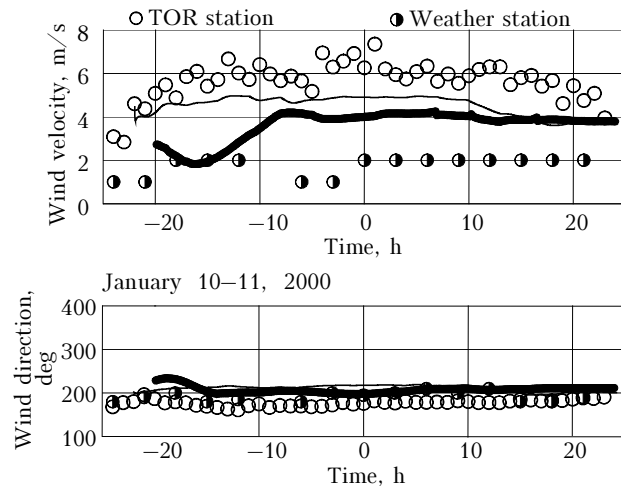
Fig. 4. Comparison of calculated and measured wind speed and direction in Tomsk on January 10–11 of 2000: data of the weather stations (half-open circles), observations at the TOR station (open circles), one-dimensional model (1)–(7) (thick solid curve), calculation by 3D mesoscale non-hydrostatic model (thin curve). Negative values on abscissa correspond to the first day of the chosen period, and positive values correspond to the second day.
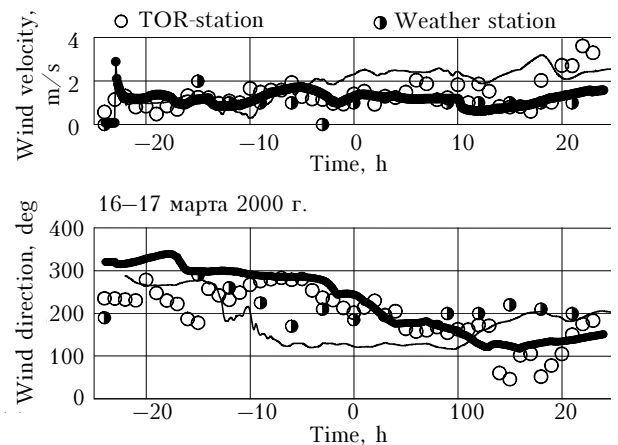
Fig. 5. Comparison of calculated and measured wind velocity and direction in Tomsk on March 16–17 of 2000. The designations are the same as in Fig. 4.

Figure 8 depicts the calculated and measured CO concentration on September 7–8 of 2000. Closed circles present the results obtained by Tomsk ecological posts located in the downtown area (Post No. 2), eastern part (Post No. 5), and northern part (Post No. 14). Solid curves show the results calculated using Euler model of pollutant transport (8) from the fields of velocity and turbulent characteristics obtained by making use of the spatial mesoscale non-hydrostatic model of the atmospheric boundary layer.[2] The dashed curves present the calculated results on the CO concentration using approximate model described above with assimilation of the observations available. Figures 9 and 10 show the dynamics of variation of the CO and NO_2 concentrations on January 10–11 of 2000 near the ecological posts of air quality observation.
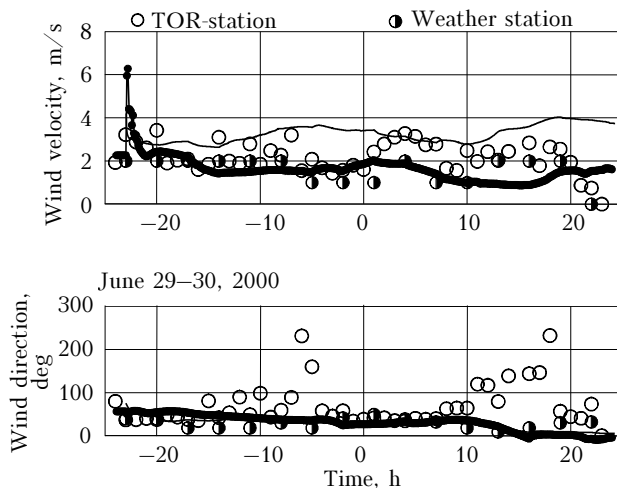
Fig. 6. Comparison of calculated and measured wind velocity and direction in Tomsk on June 29–30 of 2000. The designations are the same as in Fig. 4.
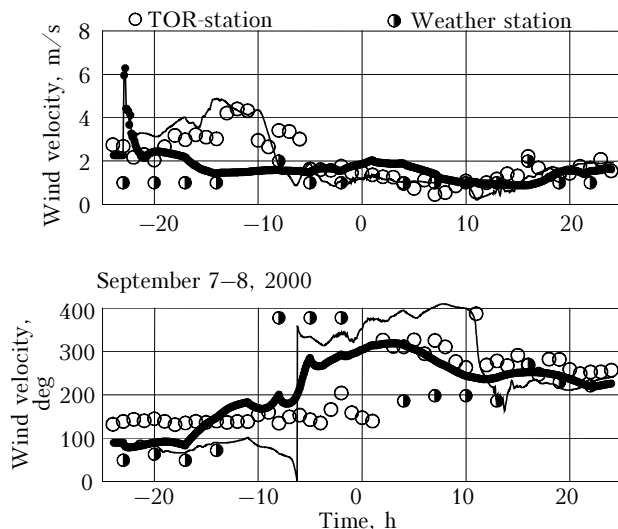
Fig. 7. Comparison of calculated and measured wind velocity and direction in Tomsk on September 7–8 of 2000. The designations are the same as in Fig. 4.

Analyzing the calculated results depicted in Figs. 4, 9, 10 and Figs. 7, 8, we can note that the wind speed and direction have a significant effect on the variation of pollution components. On January 10–11 of 2000 (see Fig. 4) the steady southwestern wind with the speed of 4–5 m/s was observed. Since the air temperature varied insignificantly in these days (from $-20°$ to $-10°$), the heat-and-power production plants worked at a constant intensity and the changes in the CO and NO_2 concentrations were largely determined by traffic emissions. The only exception is the behavior of the CO concentration at Post No. 5, which is located near powerful industrial sources of CO emissions. Therefore, there the diurnal variations of this pollutant were quite insignificant. Thus, on September 7–8 of 2000 variations of the wind direction and speed were observed (see Fig. 7).
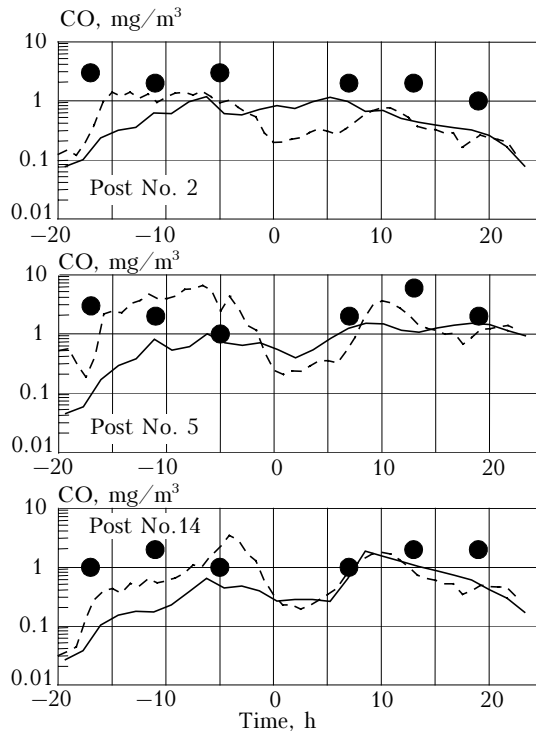
Fig. 8. Variation of the CO concentration at ecological posts in Tomsk on September 7–8 of 2000: observations (circles), calculation based on 1D empiric model (dashed curve), calculation using 3D prognostic mesoscale model (solid curve).
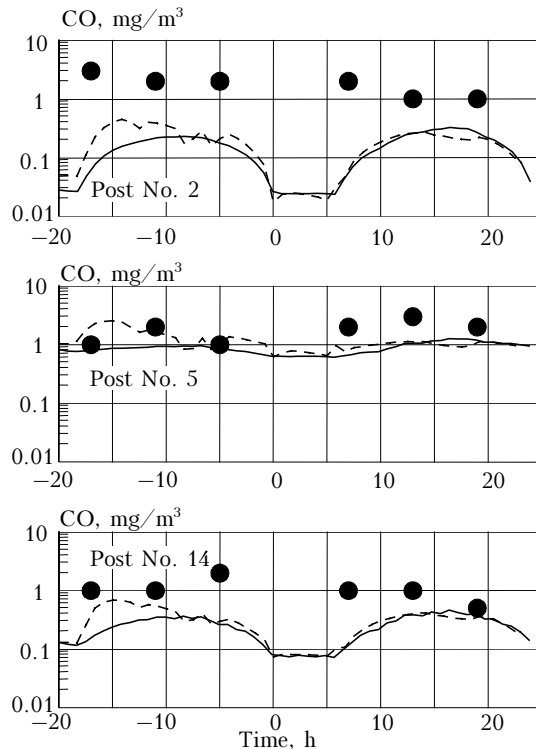
Fig. 9. Dynamics of the CO concentration at Tomsk ecological posts on January 10–11 of 2000. The designations are the same as in Fig. 8.
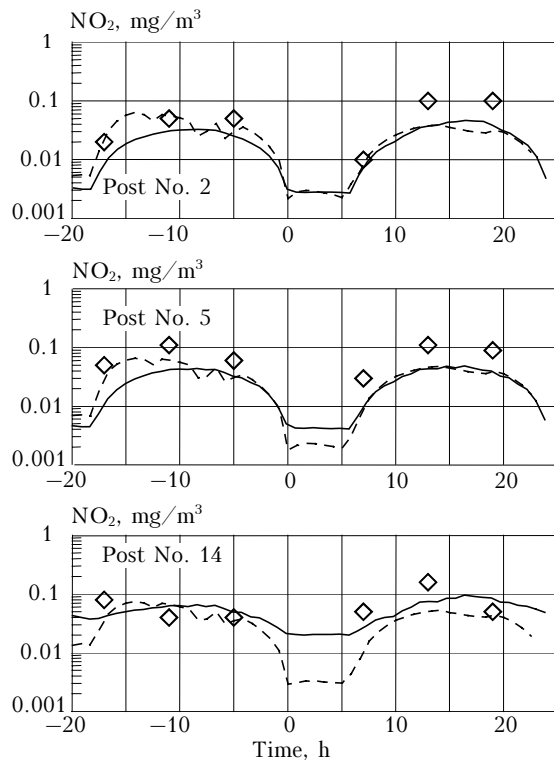
Fig. 10. Dynamics of the NO_2 concentration at Tomsk ecological posts on January 10−11 of 2000. The designations are the same as in Fig. 8.

In the evening on September 7 the wind was gentle with the speed of 1−2 m/s. Its direction slowly changed from northern to western. This behavior of the meteorological parameters caused less pronounced diurnal variations of the CO concentration (see Fig. 8). In these days the CO level in air exceeded that observed on January 10−11 of 2000, despite the heat-and-power production plants operated at an incomplete production capacity (see, for example, data of Post No. 2).

On the whole, the results of comparison can be accepted good. The lower values of the calculated CO concentration are explained by the fact that the air was sampled near highways with heavy traffic, but in the calculations the concentration near a post was considered as an average over the computational cell (500 m × 500 m × 20 m parallelepiped). Besides, the background values of the concentrations of the pollution components were assumed zero in these calculations because of their uncertainty, and this also might affect the final result.

Conclusion

Now the developed numerical model is additionally tested, the database of the sources of atmospheric pollution in Tomsk is compiled, and chemical reactions between the pollution components are determined. The developed multiprocessor computer system can be used for solution of various problems associated with the environmental protection, for example, for prediction and estimation of the urban air quality, simulation of the consequences of technogenic disasters and emergencies, determination of possible consequences from construction of industrial plants, highways, airports, etc.

References

1. J.D. Fast, L. O'Steen, and R.P. Addis, J. Appl. Meteorol. **34**, 626−649 (1995).
2. A.V. Starchenko, D.A. Belikov, and A.O. Esaulov, in: *Proc. of ENVIROMIS-2002 Conference*, Tomsk (TsNTI, 2002), pp. 142−151.
3. M.E. Berlyand, *Prediction and Regulation of Atmospheric Pollution* (Gidrometizdat, Leningrad, 1985), 448 pp.
4. J.S. Irwin, Atmos. Environ. **13**, 191−194 (1979).
5. R.T. McNide, M.D. Moran, and R.A. Pielke, Atmos. Environ. **22**, 2445−2462 (1988).
6. A.N.V. Satyanarayana, V.N. Lykossov, and U.C. Mohanty, Boundary Layer Meteorol. **96**, 393−419 (2000).
7. C.A. Sherman, J. Appl. Meteorol. **17**, 312−319 (1978).
8. A.V. Starchenko, in: *Proc. of ENVIROMIS Conference*, Tomsk (2000), pp. 77−82.
9. R. Kunz and N. Moussiopoulos, Atmos. Environ. **29**, 3375−3391 (1995).
10. P.J. Hurley, CSIRO Atmospheric Research Technical Paper No. 43 (CSIRO, Aspen dale, 1999), 39 pp.
11. V.A. Shnaidman, N.S. Brodskaya, and V.M. Losev, Tr. Gidromettsentra SSSR, Issue 238, 64−74 (1981).
12. http://infospace.meteo.ru
13. A.A. Samarskii and E.S. Nikolaev, *Methods for Solution of Grid Equations* (Nauka, Moscow, 1978), 590 pp.
14. B. Van Leer, J. Comput. Phys. **14**, 361−370 (1974).
15. A.V. Starchenko   and   A.O. Esaulov,   *Parallel Calculations on Multiprocessor Computers* (Tomsk State University Publishing House, Tomsk, 2002), 56 pp.
16. D.A. Belikov and A.V. Starchenko, in: *Abstracts of Reports at IX Workgroup on Siberian Aerosols,* Tomsk (2002), p. 46.
17. A.V. Starchenko and A.S. Karyakin, Proc. SPIE **4341**, 626−633 (2000).